



# IJRASET

International Journal For Research in  
Applied Science and Engineering Technology



---

# INTERNATIONAL JOURNAL FOR RESEARCH

IN APPLIED SCIENCE & ENGINEERING TECHNOLOGY

---

**Volume: 6      Issue: III      Month of publication: March 2018**

**DOI: <http://doi.org/10.22214/ijraset.2018.3168>**

**[www.ijraset.com](http://www.ijraset.com)**

**Call:  08813907089**

**E-mail ID: [ijraset@gmail.com](mailto:ijraset@gmail.com)**

# Application of Integral Transform to Recognition of Plastic Surgery Faces and the Surgery Types: an Approach with Volume based Scale Invariant Features and SVM

Haricharan Amarsing Dhirbasi<sup>1</sup>, Dr. Bondar Kirankumar Laxmanrao<sup>2</sup> Dr. Archana c Sable<sup>3</sup>

<sup>1</sup> Lecturer, N.E.S, Science College, S. R. T. M. University,

<sup>2</sup> Professor, Department of Mathematics., N.E.S, Science College, S. R. T.M. University, Nanded (M.S) India

<sup>3</sup> Asstt. Prof. School of Computational Sciences, S. R. T. M. University, Nanded

**Abstract:** Face recognition is one of the challenging problems which suffer from practical issues like pose, expression, and illumination changes, and/or aging. Plastic surgery is one among the issues that poses great difficulty in recognizing the faces. The literature has been reported with traditional features and classifiers for recognizing the faces after plastic surgery.

In order to reduce the computational complexity of high-dimensional feature descriptor and improve the accuracy of recognition algorithm, the paper proposes Volume based SIFT (V-SIFT) for accurate face recognition after the plastic surgery. The corresponding feature extracts the key points and volume of the scale-space structure for which the information rate is determined.

This provides least effect on uncertain variations in the face since the volume is the higher order statistical feature. The corresponding V-SIFT features are applied to the Support vector machine for classification. The normal SIFT feature extracts the key points based on the contrast of the image and the V- SIFT feature extracts the key points based on the volume of the structure.

Thus V-SIFT provide better performance when compared with PCA and normal based feature extraction.

The effectiveness of the algorithm is verified by experiments on the ORL face image database, which demonstrates good stability and robustness especially under the conditions of some confounding factors such as different facial expressions, postures and so on.

**Keywords:** Integral Transform, Face recognition, Plastic surgery, V-SIFT feature, SVM classification

## I. INTRODUCTION

In plastic surgery, rather than changing the global features, local features are often changed since they are more prominent for plastic face image. SIFT descriptors are invariant to uniform orientation, scaling and illumination changes, and hence it is even more robust to identify the objects. Moreover, SIFT descriptors are more effective over other contemporary local descriptors on structured as well as textured image.

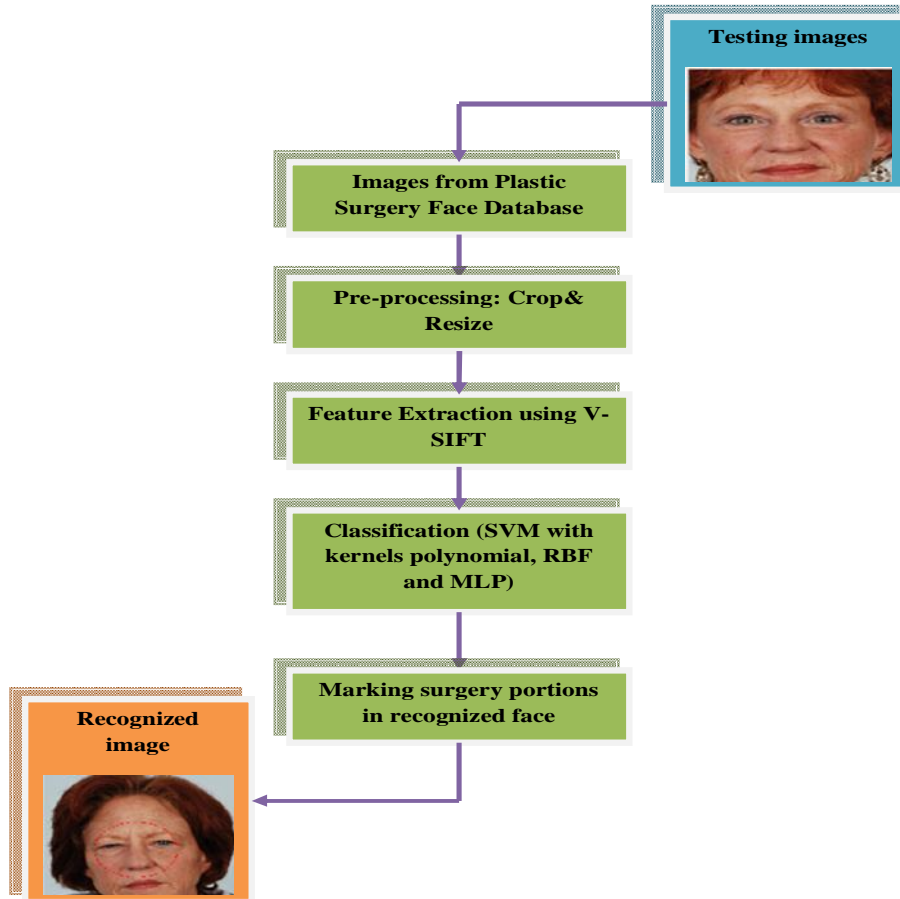


Fig 1: Block diagram of V-SIFT based plastic surgery face recognition

In the proposed methodology as in Fig 1, the testing image  $I^T$  from the plastic surgery face database is initially processed under pre-processing for image enhancement, where it crops and resized. Next to this, the features are extracted from the pre-processed image  $I^P$  with the aid of V-SIFT. Then the classification process is done using SVM classifier and results the recognized image.

## II. SIFT DESCRIPTOR

The architecture diagram of the SIFT descriptor is illustrated in Fig 2. The comprised computations of the SIFT descriptor is as follows:

(i) Detection of Scale-space extrema: Here, a scale space is constructed for the detection of the image's blob structures, in which the interest points named key points are detected. The scale space utility is generated from the convolution of variable scale Gaussian  $GU(u, v, \tau^2)$  using  $I^T(u, v)$ , which is defined in Eq. (1). Moreover, the true scale invariance is acquired from the  $\tau^2 \nabla^2 GU$  along with  $\tau^2$  factor. Hence, the selection of scale is done automatically by convolution with Laplacian function  $H(u, v, \tau^2)$ , which is defined in Eq. (2).

$$H(u, v, \tau^2) = GU(u, v, \tau^2) * I^T(u, v) \tag{1}$$

$$P(u, v, \tau^2) = \tau^2 \nabla^2 GU * I^T(u, v) = \tau^2 \nabla^2 H(u, v, \tau^2) \tag{2}$$

if there is any closer relation between scale of the image and  $\sigma$  value of Laplacian, the result  $P(u, v, \tau^2)$  is formulated by convolving the corresponding image with  $\tau^2 \nabla^2 GU$ , and it will be considered as extremum. Hence for the blob detection and optimal scale representation, the points those are extrema in scale as well as spatial spaces are chosen.

(ii) Removal of unreliable key points: This is the second step; here the formulation of  $P(u, v, \tau^2)$  at all the key points is done. Once the formulation is completed, it is checked for whether the value is below the threshold. If so, then it means that the attained structure has less contrast (which is more sensitive to noise), then the corresponding key point will be detached. Further, for weak peaks in the normalized Laplacian of Gaussian, the formulation of the primary curvature ratio of every candidate is done and checks whether the ratio is below the threshold, if so, then the key point remains.

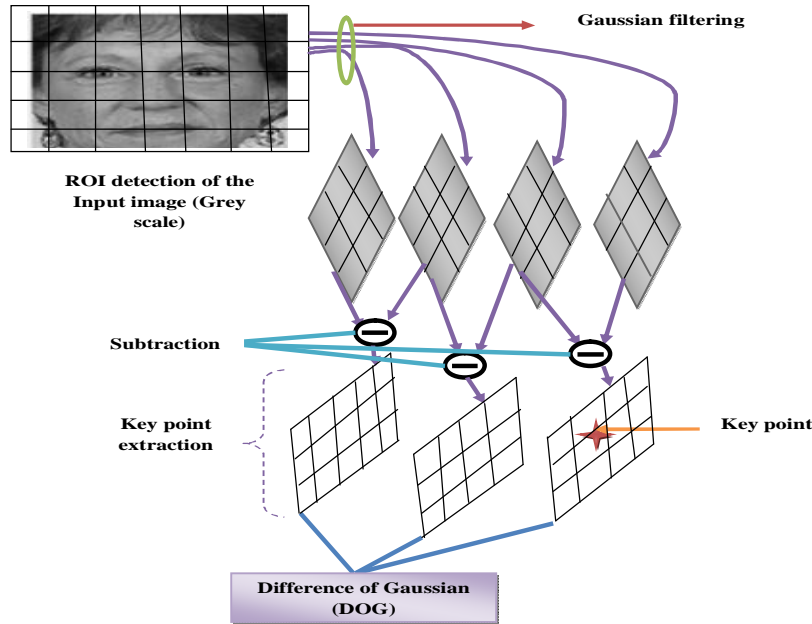


Fig. 2: Architecture diagram of SIFT descriptor

(iii) Assigning Orientation: Here, the key point is assigned in one or more orientations with the basis of gradient directions of local image.

(iv) Key point descriptor: Basically, around the key point location, all the gradient magnitude and orientations of the image are sampled and utilizes the key point's scale for choosing the Gaussian blur's level. Then the formulation of the feature descriptor is carried out as a set of 16x16 pixels are round the key points. 8 bins are present in every histogram and 4x4 array of histograms are compiled in each descriptor, and that are around the key point. Hence the feature vector of each key point will be  $4 \times 4 \times 8 = 128$  dimension, which is diagrammatically represented in Fig 3.3

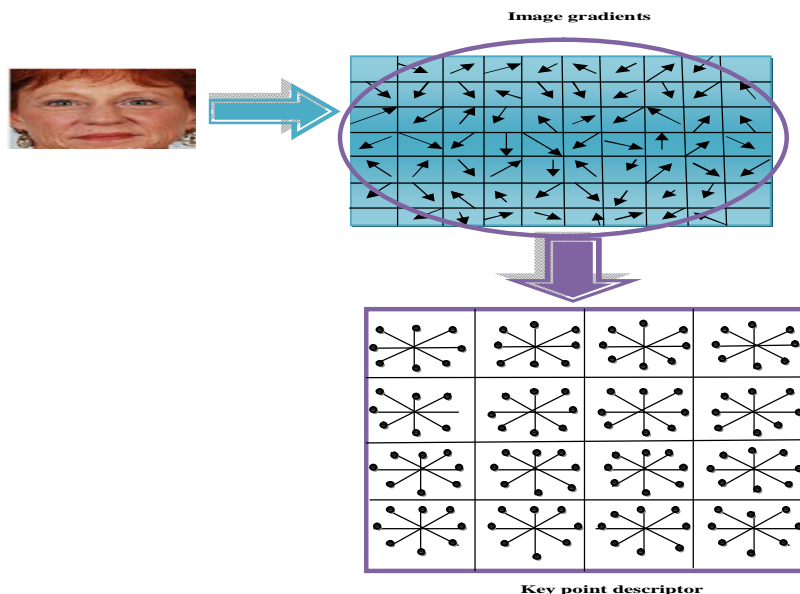


Fig. 3: Key point descriptor of the SIFT descriptor

### III.3.3 V-SIFT DESCRIPTOR

Generally, the Difference of Gaussian (DOG) in SIFT features has varied gains. When the noise is supplemented to the image or if the image is blurred, then the stability of the features that are extracted is not so effective. Thus to get the perfect matching, it is essential to extract the stable feature points. DOG is utilized to capture the scale invariant features and the establishment of DOG scale space  $DG(u, v, \tau)$  is done by scale space function, which is defined in Eq. (3) and (4).

$$DG(u, v, \tau) = H(u, v, k\tau) - H(u, v, \tau) \tag{3}$$

$$DG(u, v, \tau) = GU(u, v, k\tau) - GU(u, v, \tau) * I^T(u, v) \tag{4}$$

where  $GU(u, v, \tau) = \frac{1}{2\tau^2} e^{-\frac{(u^2+v^2)}{2\tau^2}}$  determines the Gaussian function in the Eq.(4). In this DOG scale space, the entire sample points are compared with 26 neighbours for the identification of 2D image space along with intense points. For any image, the target point must be compared to 8 and 18 neighbours in both the below and above scale. The formulation of true scale is carried out from  $\tau^2 \Delta^2 GU$  with  $\tau^2$ . Subsequently, the convolution is attained with the normalized Laplacian function and the scale selection is accomplished as defined in Eq.(2). In this algorithm, the operator named scale normalized Laplacian operator is utilized for the selection of scale. Let us consider a model configuration: A Gaussian function as given in Eq. (5) is a 2D blob model that characteristics  $\tau_1$  length in any coordinates direction.

$$I^T(u, v) = GU(u, v, \tau_1^2) = e^{-\frac{(u^2+v^2)}{2\tau_1^2}} \tag{5}$$

Further, the scale space demonstration of  $I^T$  is followed from the Gaussian property, which is termed as semi group property,  $GU(u, v, \tau_X^2) * GU(u, v, \tau_Y^2) = GU(u, v, \tau_X^2 + \tau_Y^2)$  and the representation is defined in Eq. (6)

$$H(u, v, \tau^2) = GU(u, v, \tau_1^2 + \tau^2) \tag{6}$$

With the aid of Eq. (2), after certain algebraic influences, it could be revealed that for  $\sigma > 0$ , there is a distinctive over scale as defined in Eq. (7), this supreme over scales is defined as given in Eq.(8). Therefore, the scale that lies in the scale space supreme shows the characteristic size of the particular blob, which is the rationale behindhand, the detection of the scale space. It is well known that a second order Laplacian operator is highly sensitive to noise and hence the unreliable key points are eliminated by the next step, 'unreliable key point removal'.

$$|P(0,0, \tau^2)| = |\tau^2 \nabla^2 H(0,0, \tau^2)| = \frac{\tau^2}{\Pi(\tau_1^2 + \tau^2)^2} \tag{7}$$

$$\partial_\tau (\tau^2 \nabla^2 H(0,0, \tau^2)) = 0 \iff \tau = \tau_1 \tag{8}$$

Here, initially, the formulation of  $|P(u, v, \tau^2)|$  is done for all the location of every candidate and if the obtained value is below the threshold, then the key point is detached. For instance, let the Gaussian blob structures be  $I_1^T(u, v, \tau_1^2)$  and  $I_2^T(u, v, \tau_2^2)$  with varied scales  $\tau_1 = 10$  and  $\tau_2 = 50$ , which is shown in Fig 5. Once the convolution is done with  $\tau^2 \nabla^2 GU$  and results in 1D outputs of  $I_1^T$  and  $I_2^T$ , which is illustrated in Fig 6.

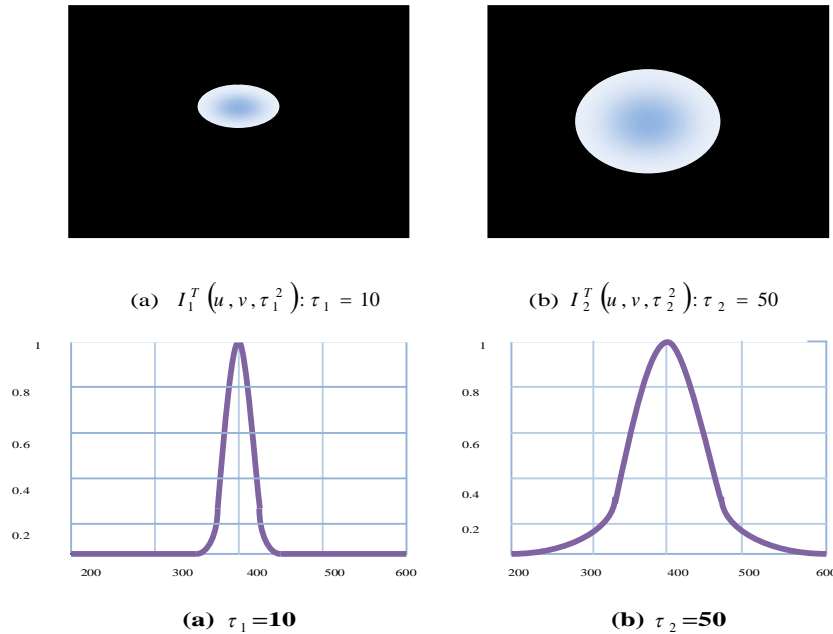


Fig 5: Gaussian blob with varied scales and their respective 1D representation

Further, the key points that represent the blobs are distinguished at  $P_1$  and  $P_2$  extrema. If both  $|P_1(u, v, \tau_1^2)|$  and  $|P_2(u, v, \tau_2^2)|$  extrema are same as shown in Fig 6, then in the algorithm, both  $I_1^T$  and  $I_2^T$  are similarly treated. Both of them will be either kept or removed.

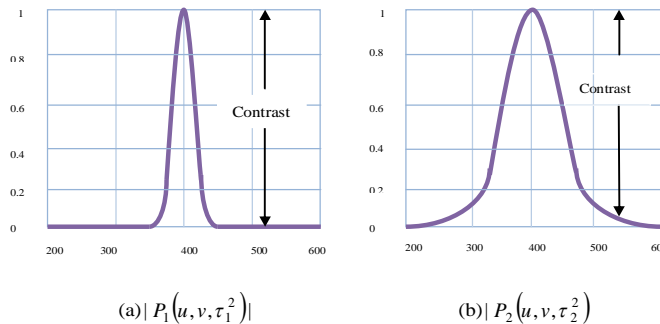


Fig. 6: Output of  $I_1^T$  and  $I_2^T$

However, if both  $I_1^T$  and  $I_2^T$  are varied structures with diverse scales as represented in Fig. 5, then they have not be considered as useful or useless equally. If  $I_2^T$  is greater than  $I_1^T$ , then it is determined that  $I_2^T$  is fewer sensitive to noise but  $I_1^T$  is more sensitive to noise. The key points that represents  $I_2^T$  must be kept and at the same time the key points which denotes  $I_1^T$  must be removed. Hence VSIFT is the contrast approach that has the module of eliminating irrelevant key points, which are based on volume of the structure, which is defined as per Eq. (9).

$$L(u, v, \tau^2) = \tau^2 |P(u, v, \tau^2)| = \tau^4 |\nabla^2 GU * I^T(u, v)| \tag{9}$$

where  $\tau$  denotes scale of the key point. We can also derive Eq. (10) and (11) from Eq. (9). Even though the extrema of both  $|P_1(u, v, \tau_1^2)|$  and  $|P_2(u, v, \tau_2^2)|$  are similar, the extrema of  $L_1(u, v, \tau_1^2)$  and  $L_2(u, v, \tau_2^2)$  are different from each other. Here the case is determined in Eq. (12).

$$L_1(u, v, \tau_1^2) = \tau_1^2 |P_1(u, v, \tau_1^2)| \tag{10}$$

$$L_2(u, v, \tau_2^2) = \tau_2^2 |P_2(u, v, \tau_2^2)| \tag{11}$$

$$L_1(u, v, \tau_1^2)_{\text{extrema}} < L_2(u, v, \tau_2^2)_{\text{extrema}} \tag{12}$$

The value of  $L(u, v, \tau^2)$  is formulated in the locality of every candidate key point, and if the value goes below the threshold given, then the key point must be removed or else it should be remained.

#### IV. SVM RECOGNITION SYSTEM

The basic concept of SVM is diagrammatically illustrated in Fig 3.6. It shows the hyperplane that separates the classes and has the largest margin between support vectors. SVM is a machine learning structure from data or information. It is important to learn the mapping strategy:  $A \rightarrow B$ , where  $a \in A$  is some object and  $b \in B$  is denoting the class label. For instance, consider the 2-class classification. Therefore,  $a \in R^n$ ,  $b \in \{\pm 1\}$ , where  $R$  denotes the radius and  $n$  defines the number of pixels in the image.

##### A. Training Sets with Prediction Modalities

let us consider the input set  $A$  and output set  $B$ . The training set for the input and output sets be  $(a_1, b_1), \dots, (a_m, b_m)$ . By giving  $a \in A$ , the suitable  $b \in B$  must be found, which means the classifier must be learned:  $f(a, \alpha)$ , where  $\alpha$  denote the parameter of the function  $f$ .

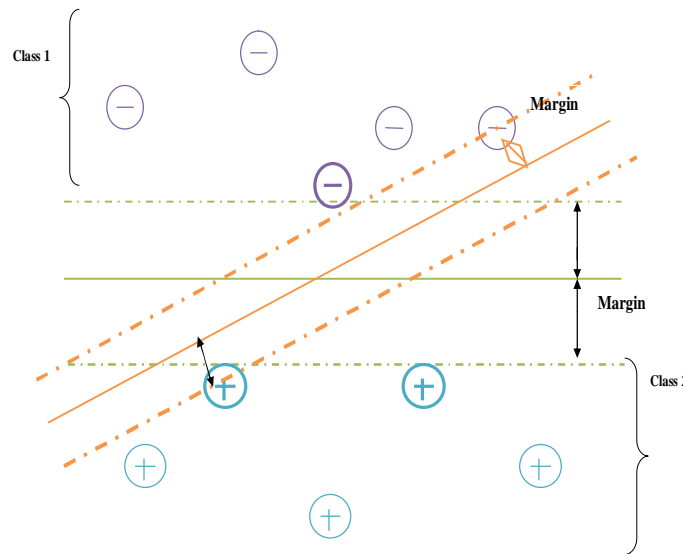


Fig. 7: Basic concept of SVM

For instance, if the modality is selected from the set of hyperlanes in  $R^n$ : then the function of SVM classifier is defined in Eq.(13), where  $S$  denotes the bias that given to the classifier and represents the weight vector.

$$f(a, (e, s)) = \text{sign}(e \cdot a + s) \tag{13}$$

##### B. Empirical and True Risk

$f(a, \alpha)$  is learned by selecting the appropriate function, which outperforms on the training data, the empirical risk  $K^{emp}$  is defined in Eq. (14), where  $o$  represents the zero-one loss function,  $o(b, \hat{b}) = 1$ , if  $b \neq \hat{b}$  and 0 otherwise. By learning this, the overall risk is reduced, which is defined in eq. (15), where  $O(a, b)$  refers the indefinite joint distribution function of  $a$  and  $b$ .

$$K^{emp}(\alpha) = \frac{1}{m} \sum_{i=1}^m o(f(a_i, \alpha), b_i) = \text{Training error} \tag{14}$$

$$K(\alpha) = \int o.(f(a, \alpha)b)O(a, b) = \text{Test error} \tag{15}$$

### C. Hyperlane's Capacity

The hyperlane  $(e \cdot a) = 0$  is considered, where  $e$  is normalized in terms of set of points  $A^*$ , such that  $\min_i |e \cdot a_i| = 1$ , and  $\|e\|^2$  is minimized to have low capacity, the reduction is correspondent to the gaining of large margin classifier. The diagrammatic representation is shown in Fig 7.

4. *Linear Support Vector Machine*: The function must be find to minimize the objective such as Training error and complexity, it can be defined as given in Eq.( 16). Consider a set of hyperplane  $f(a) = (e \cdot a) + s$  to minimize the objective  $\min_i |e \cdot a_i| = 1$ , which is defined in Eq. (17).

$$\frac{1}{m} \sum_{i=1}^m o(f(a_i, \alpha), b_i) + \text{Complexity} \tag{16}$$

$$\frac{1}{m} \sum_{i=1}^m o(e \cdot a_i + s, b_i) + \|e\|^2 \tag{17}$$

In our work, the obtained V-SIFT feature descriptor of the plastic surgery is given to SVM classifier, which aims to find the decision exterior that has the supreme distance to the point of varied classes. The formulation of SVM classifier is defined in Eq.(3.8).

$$SV = e \cdot I_f^T + s \tag{18}$$

where  $I_f^T$  denotes the features extracted using V-SIFT feature descriptor,  $s$  is the bias that applied to classifier and  $e$  represents the weight vector. In Eq.(18),  $e \cdot I_f^T + s = -1$  signifies the negative support vectors and  $e \cdot I_f^T + s = +1$  signifies the positive support vectors respectively. This method objects to distinguish the faces that have been imperilled to the plastic surgery, which owe to great ambiguity in the faces after and before surgery.

## V. RESULTS AND DISCUSSION

In this section, the result comparison of both the SIFT and V-SIFT feature descriptor are shown clearly. Fig 8 shows the original images. For each original image, the corresponding vertical edge and horizontal edge of the image was evaluated and it is illustrated in Fig. 9 and 10. The gradient magnitude of the images is also shown in Fig. 11. Similarly, the theta images of the given input images are illustrated in Fig. 12.

**SIFT feature descriptor**: In this descriptor, the SIFT array is constructed, which is based on the key points that are selected from the input image. For instance, consider the image 1 in Fig 8, if we choose 850 key points from the input image, then the SIFT array might be  $[850 \times 128]$ , which means that for each key points, 128 descriptors are generated. Then the array is diminished to the size of  $[25 \times 25]$  and from this, the SIFT contour, SIFT grid are evaluated. The SIFT contour and SIFT grid SIFT surf of all the given input images are illustrated in Fig. 13 and 14 respectively.

**V-SIFT feature descriptor**: The process of V-SIFT descriptor is same as the SIFT descriptor, but the difference is that V-SIFT descriptor evaluates the features by including the volume of the structure whereas the SIFT descriptor does not includes the volume. In this developed recognition system, V-SIFT is used to extract the features. The V-SIFT contour and V-SIFT grid are evaluated for the given input images and it is illustrated in Fig. 15 and 16 respectively. While comparing both the feature descriptor, it is found that V-SIFT descriptor has provided promising results with better feature extraction.



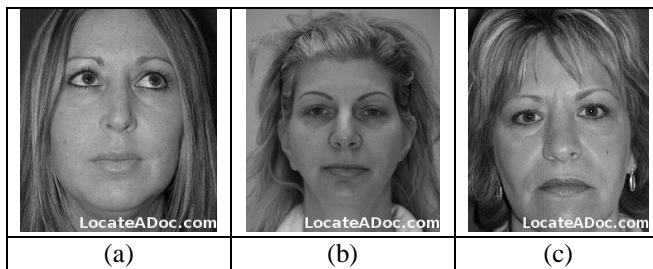


Fig. 8: Original images (a) Image 1 (b) Image 2 (c) Image 3

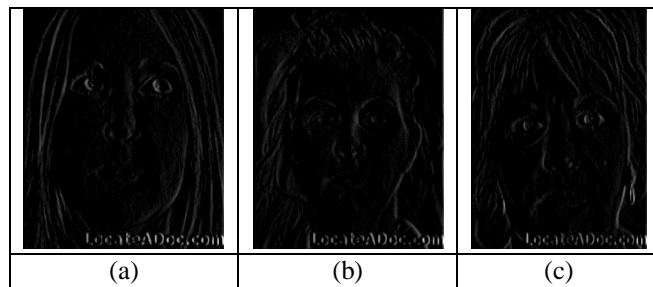


Fig. 9: Vertical edge of the given images (a) Image 1 (b) Image 2 (c) Image 3

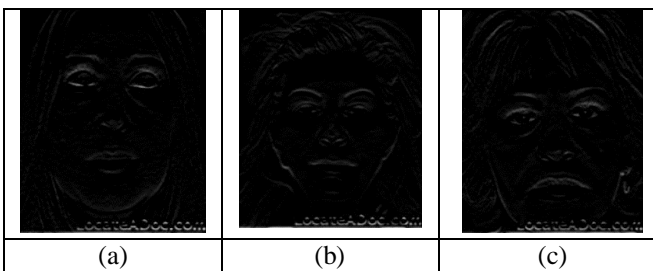


Fig. 10: Horizontal edge of the given images (a) Image 1 (b) Image 2 (c) Image 3

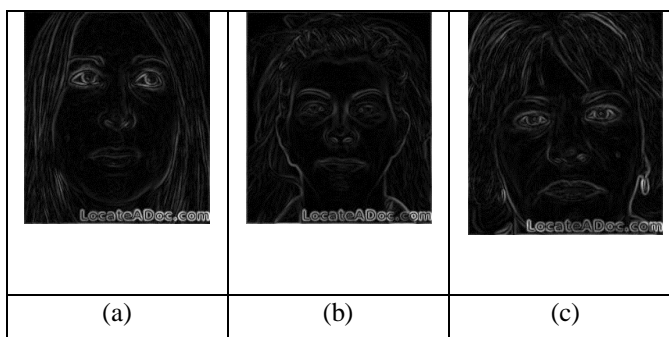


Fig. 11: Gradient magnitude of the images (a) Image 1 (b) Image 2 (c) Image 3

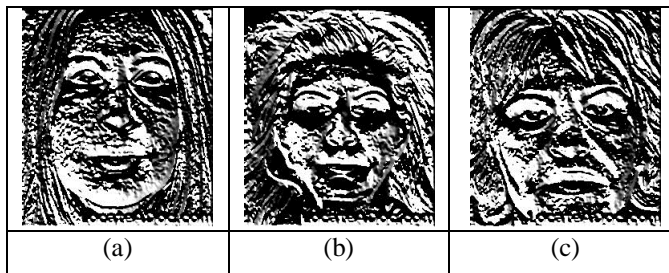


Fig. 12: Theta representation of the images (a) Image 1 (b) Image 2 (c) Image 3

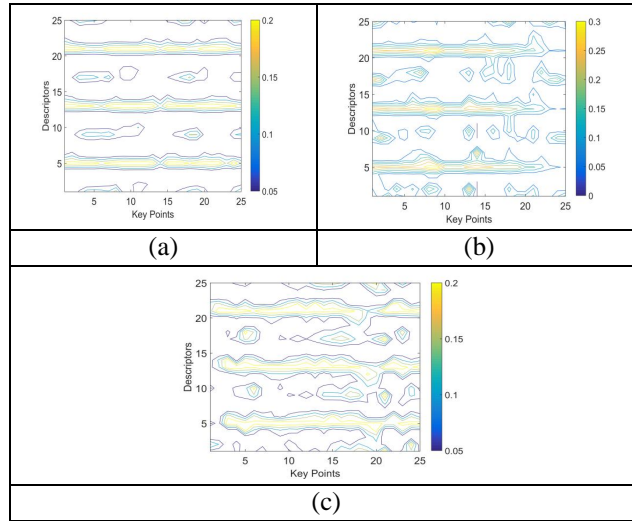


Fig. 13: SIFT contour of images (a) Image 1(b) Image 2 (c) Image 3

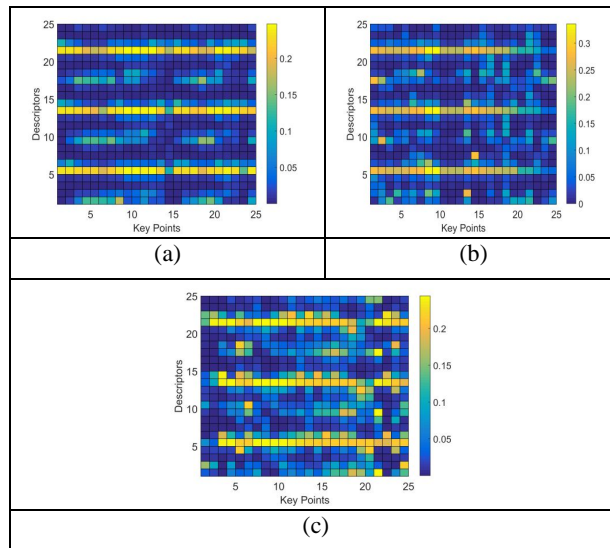


Fig. 14: SIFT grid of the images (a) Image 1(b) Image 2 (c) Image 3

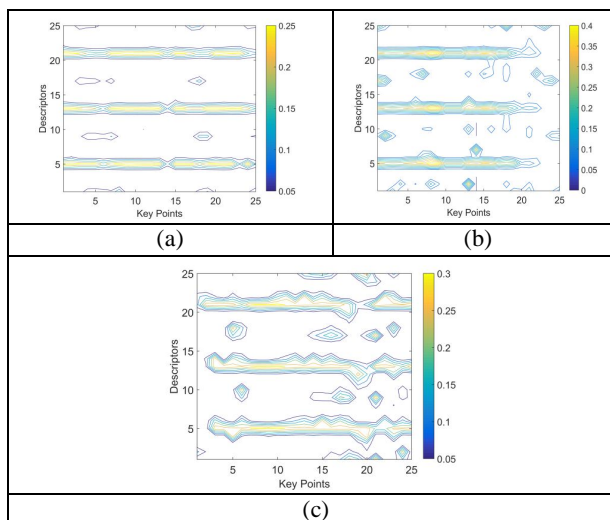


Fig. 15: V-SIFT contour of the images (a) Image 1(b) Image 2 (c) Image 3

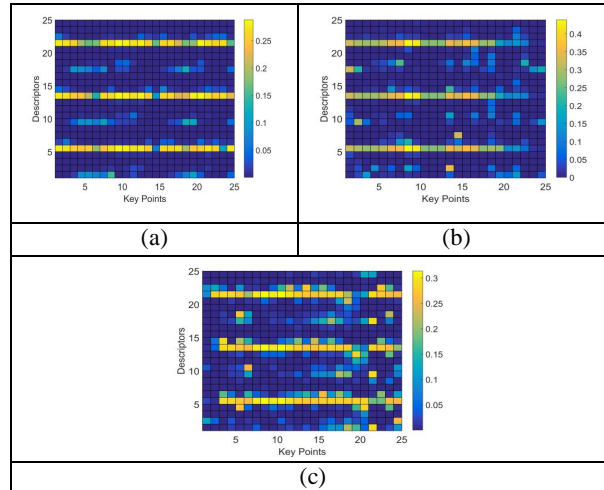


Fig. 16: VSIFT grid of the images (a) Image 1(b) Image 2 (c) Image 3

**A. Statistical Analysis**

The statistical analysis of the plastic surgery face recognition describes the comparison of features such as Principle Component Analysis (PCA), SIFT and the proposed method Volume SIFT. The performance measures are analysed for all these features. The analysis of the classifiers such as linear SVM, quadratic SVM, RBF SVM and MLP SVM for before and after plastic surgery is illustrated in table 1,2,3 & 4. The ranking of each measure is mentioned in bracket. The definitions all the measures are based on the Wikipedia source.

In the source, accuracy determines the degree of correctly classified face. Sensitivity is the measure of the method to correctly identify the positive samples while the specificity is the measure of the method to correctly identify the negative samples. Precision can give the ratio of positive against all the positive results. FPR, FNR, NPV and FDR can correctly predict the incorrect identification and correct identification. The correctness of the classification algorithm and the efficacy of binary class classification can be determined by F1\_Score and MCC. In table 1 and 2, which is the linear SVM and quadratic SVM, the accuracy is better for the PCA while the sensitivity and the specificity are better for the V-SIFT feature for plastic surgery faces. But here all the measures are better for the V-SIFT feature. The ranking of all the measures is calculated and the final rank is best for EV SIFT feature when compared to the other feature extraction methods in linear SVM and quadratic SVM. In table 3, it describes the analysis for RBF SVM. Here all the measures are better for PCA, SIFT AND V-SIFT while the proposed EV-SIFT feature shows less performance. By analysing the rank, PCA is better than other methods in RBF SVM. In table 4, all the measures show better performance while using V-SIFT feature. Other feature extraction methods show poor performance. So by examining the overall analysis, it is clear that the V-SIFT feature extraction is better for the plastic surgery face recognition purpose.

TABLE1. EXPERIMENTAL EVALUATION ON SVM WITH LINEAR KERNEL FUNCTION

	PCA	SIFT	VSIFT
Accuracy	0.66(3)	0.80(2)	0.93(1)
Sensitivity	0.17(3)	0.20(2)	0.17(1)
Specificity	0.94(1)	0.97(2)	0.96(3)
Precision	0.2 (1)	0.6(2)	0.53(3)
FPR	0.06(3)	0.03(2)	0.04(1)
FNR	0.82(3)	0.80(2)	0.83(1)
NPV	0.94(3)	0.97(2)	0.96(1)
FDR	0.8 (3)	0.4 (2)	0.47(1)
F1_Score	0.19(3)	0.30(2)	0.26(1)
MCC	0.13(3)	0.26(2)	0.22(1)
Avg_rank	3.5	2	1.2
Final_rank	3	2	1

TABLE 2. EXPERIMENTAL EVALUATION ON SVM WITH QUADRATIC KERNEL FUNCTION

	PCA	SIFT	VSIFT
Accuracy	0.88(3)	0.83(2)	0.93(1)
Sensitivity	0.13(3)	0.07(1)	0.13(2)
Specificity	0.94(3)	0.93(2)	0.94(1)
Precision	0.2 (3)	0.07(1)	0.27(2)
FPR	0.06(3)	0.07(2)	0.06(1)
FNR	0.87(3)	0.93(1)	0.88(2)
NPV	0.94(3)	0.93(2)	0.94(1)
FDR	0.8(3)	0.93(2)	0.73(1)
F1_Score	0.16(3)	0.07(2)	0.17(1)
MCC	0.09(3)	0(1)	0.10(2)
Avg_rank	2.8	2.2	1.4
Final_rank	3	2	1

TABLE 3. EXPERIMENTAL EVALUATION ON SVM WITH RBF KERNEL FUNCTION

	PCA	SIFT	VSIFT
Accuracy	0.78(3)	0.83(2)	0.93(1)
Sensitivity	0.07(1)	0.13(2)	0.13(2)
Specificity	0.93(1)	0.94(2)	0.94(2)
Precision	0.07(1)	0.27(2)	0.2 (3)
FPR	0.07(2)	0.06(1)	0.06(1)
FNR	0.93(3)	0.88(2)	0.87(1)
NPV	0.93(1)	0.94(2)	0.94(2)
FDR	0.93(3)	0.83(2)	0.8(1)
F1_Score	0.07(3)	0.17(2)	0.16(1)
MCC	0(3)	0.09(1)	0.09(1)
Avg_rank	3.7	2.4	2.1
Final_rank	3	2	1

TABLE 4. EXPERIMENTAL EVALUATION ON SVM WITH MLP KERNEL FUNCTION

	PCA	SIFT	VSIFT
Accuracy	0.78(3)	0.83(2)	0.93(1)
Sensitivity	0.07(1)	0.13(2)	0.13(2)
Specificity	0.93(1)	0.94(2)	0.94(2)
Precision	0.07(1)	0.27(2)	0.2 (3)
FPR	0.07(2)	0.06(1)	0.06(1)
FNR	0.93(3)	0.88(2)	0.87(1)
NPV	0.93(1)	0.94(2)	0.94(2)
FDR	0.93(3)	0.83(2)	0.8(1)
F1_Score	0.07(3)	0.17(2)	0.16(1)
MCC	0(3)	0.09(1)	0.09(1)
Avg_rank	3.7	2.4	2.1
Final_rank	3	2	1

## VI. CONCLUSION

This paper has presented a face recognition technique that uses derived features based on V-SIFT approach. The corresponding system was evaluated using plastic surgery image database of 15 subjects where it contains each image of pre-surgery and post surgery faces. The proposed V-SIFT approach has obtained the volume of the structure and the contrast of the image and also it has removed all the unwanted key points effectively. The extracted features were applied to the SVM classifier for the recognition purpose. The performance measures were analyzed in different kernel of SVM with different existing features. Here V-SIFT feature was effective for producing the best performance. The parameters of SVM classifier such as radius and enlarge factor was varied. From the analysis it was clear that, the performance was better for varied values of radius and EF and it was not fixed. So here a proper tuning was needed for obtaining the fixed value. In future work, the analysis based on the tuning process will be done to have the accurate recognition of plastic surgery face.

## REFERENCES

- [1] Anil Kumar Sao and B. Yegnanarayana, "Face Verification Using Template Matching", IEEE Transactions on Information Forensics and Security, vol. 2, no. 3, pp. 636-641, Sep. 2007.
- [2] William Robson Schwartz, Huimin Guo, Jonghyun Choi and Larry S. Davis, "Face Identification Using Large Feature Sets", IEEE Transactions on Image Processing, vol. 21, no. 4, pp. 2245-2255, April 2012.
- [3] M. A. Turk and A. P. Pentland, "Face recognition using eigenfaces", In Proceedings of the IEEE Computer Society Conference on Computer Vision and Pattern Recognition, Maui, HI, 1991, pp. 586- 591.
- [4] J. Ruiz-del-Solar and P. Navarrete, "Eigenspace-based face recognition: a comparative study of different approaches", IEEE Transactions on Systems, Man, and Cybernetics, Part C (Applications and Reviews), vol. 35, no. 3, pp. 315-325, Aug. 2005.
- [5] S. Lawrence, C. L. Giles, Ah Chung Tsoi and A. D. Back, "Face recognition: a convolutional neural-network approach", IEEE Transactions on Neural Networks, vol. 8, no. 1, pp. 98-113, Jan.1997.
- [6] Xiaofei He, Shuicheng Yan, Yuxiao Hu, P. Niyogi and Hong-Jiang Zhang, "Face recognition using Laplacianfaces", IEEE Transactions on Pattern Analysis and Machine Intelligence, vol. 27, no. 3, pp. 328-340, March 2005.
- [7] Tolga Inan and Ugur Halici, "3-D Face Recognition With Local Shape Descriptors", IEEE Transactions on Information Forensics and Security, vol. 7, no. 2, pp. 577-587, April 2012.
- [8] Ze Lu, Xudong Jiang and Alex C. Kot, "A Color Channel Fusion Approach for Face Recognition", IEEE Signal Processing Letters, vol. 22, no. 11, pp. 1839-1843, Nov. 2015.
- [9] Yong Xu, Xiaozhao Fang, Xuelong Li, Jiang Yang, Jane You, Hong Liu and Shaohua Teng, "Data Uncertainty in Face Recognition", IEEE Transactions on Cybernetics, vol. 44, no. 10, pp. 1950-1961, Oct. 2014.
- [10] Anil K. Jain, Brendan Klare and Unsang Park, "Face recognition: Some challenges in forensics", 2011 IEEE International Conference on Automatic Face & Gesture Recognition and Workshops (FG 2011), Santa Barbara, 2011, pp. 726- 733.
- [11] Poonam Sharma, Ram N. Yadav and Karmveer V. Arya, "Pose- invariant face recognition using curvelet neural network", IET Biometrics, vol. 3, no. 3, pp. 128-138, Sep. 2014.
- [12] Sang-Heon Lee, Dong-Ju Kim and Jin-Ho Cho, "Illumination-robust face recognition system based on differential components", IEEE Transactions on Consumer Electronics, vol. 58, no. 3, pp. 963-970, Aug 2012.
- [13] Wilman W. W. Zou and Pong C. Yuen, "Very Low Resolution Face Recognition Problem", IEEE Transactions on Image Processing, vol. 21, no. 1, pp. 327-340, Jan 2012.
- [14] Unsang Park, Yiyong Tong and Anil K. Jain, "Age-Invariant Face Recognition", IEEE Transactions on Pattern Analysis and Machine Intelligence, vol. 32, no. 5, pp. 947-954, May 2010.
- [15] Sivaram Prasad Mudunuri and Soma Biswas, "Low Resolution Face Recognition Across Variations in Pose and Illumination", IEEE Transactions on Pattern Analysis and Machine Intelligence, vol. 38, no. 15, pp. 1034-1040, May 2016.
- [16] Richa Singh, Mayank Vatsa and Afzel Noore, "Effect of plastic surgery on face recognition: A preliminary study", 2009 IEEE Computer Society Conference on Computer Vision and Pattern Recognition Workshops, Miami, FL, 2009, pp. 72- 77.
- [17] Richa Singh, Mayank Vatsa, Himanshu S. Bhatt, Samarth Bharadwaj, Afzel Noore and Shahin S. Nooreydzan, "Plastic Surgery: A New Dimension to Face Recognition", IEEE Transactions on Information Forensics and Security, vol. 5, no. 3, pp. 441- 448, Sep. 2010.
- [18] Xin Liu, Shiguang Shan and Xilin Chen, "Face Recognition after Plastic Surgery: A Comprehensive Study", Computer Vision – ACCV 2012, Lecture Notes in Computer Science, Springer, vol. 7725, pp. 565-576.
- [19] Maria De Marsico, Michele Nappi, Daniel Riccio and Harry Wechsler, "Robust Face Recognition after Plastic Surgery Using Local Region Analysis", Image Analysis and Recognition, Lecture Notes in Computer Science, Springer, vol. 6754, pp. 191-200.
- [20] N. S. Lakshmi Prabha and S. Majumder, "Face recognition system invariant to plastic surgery", 2012 12th International Conference on Intelligent Systems Design and Applications (ISDA), Kochi, 2012, pp. 258-263.
- [21] N. S. Lakshmi Prabha, J. Bhattacharya and S. Majumder, "Face recognition using multimodal biometric features", in Proceedings of the 2011 International Conference on Image Information Processing (ICIIP), Himachal Pradesh, 2011, pp. 1-6.



10.22214/IJRASET



45.98



IMPACT FACTOR:  
7.129



IMPACT FACTOR:  
7.429



# INTERNATIONAL JOURNAL FOR RESEARCH

IN APPLIED SCIENCE & ENGINEERING TECHNOLOGY

Call : 08813907089  (24\*7 Support on Whatsapp)